Treatment of Automotive Paint Wastewater: Photocatalytic degradation of methylene blue using semi-conductive ZrO₂

Mustafa Seyrek[1*], Filiz Boran[2] and Merve Okutan[2]

0000-0001-5386-4804, 0000-0002-4315-9949, 0000-0002-3110-0675

[1] Vocational School of Technical Sciences, Hitit University, Çorum, Turkiye
[2] Department of Chemical Engineering, Faculty of Engineering, Hitit University, Çorum, Turkiye

Abstract

Addressing water pollution, particularly in the automotive industry's painting processes, is vital due to its significant environmental impact, and the use of photocatalysis, an environmentally friendly and energy-efficient advanced oxidation method, holds promise for removing non-biodegradable organic dyes from wastewater. In this study, the use of semiconductor ZrO_2 nanoparticles in the photocatalytic degradation of pollutants in wastewater under UV light was investigated. Zeta potential, Brunauer–Emmett–Teller (BET) surface area and UV-Vis absorption spectroscopy analyzes were performed on the ZrO_2 nanoparticle synthesized under optimized experimental conditions. ZrO_2 nanoparticles synthesized under the optimized experimental conditions exhibited a high specific surface area ($51.793 \ m^2/g$). ZrO_2 nanoparticles had strong absorption in the visible light region, and the energy band gap was estimated to be approximately 3.062 eV. Photocatalytic activity was evaluated by degradation of methylene blue under UV light (366 nm). The effects of parameters such as the amount of catalyst, concentration and pH of the dye solution, the wavelength of the UV light source used (366 and 254 nm) and the type of test environment on the removal efficiency of methylene blue were investigated. ZrO_2 nanoparticles showed high degradation efficiency of 91% in a strong alkaline environment, which may be the result of the facilitated formation of –OH radicals due to the increased concentration of hydroxyl ions.

Keywords: Automotive Paint Wastewater; Paint degradation; Photocatalytic activity; Zirconia

1. Introduction

Pollution and the search for solutions to these threats are not new concerns. With industrialization and population growth, the management of environmental problems has long been a challenge for humankind, in terms of both rising energy consumption and the ever-growing amounts of waste. In addition to the increasing amount of different types of waste, the improper disposal of this waste into the environment poses a serious threat to the environment. Among these, water pollution is a major problem that needs to be controlled because water is one of the most basic needs of all life forms and our world has limited potable water resources [1–5]. It is reported in the literature that more than half of the environmental impact of the automotive industry, whose production volume is increasing day by day, is caused by painting and coating processes. During the painting process, paint wastewater is generated from paint overspray on the car surface, rinsing chemicals and equipment washing. It is therefore important to investigate, develop and implement alternative treatment methods to improve water quality and enable its reuse [6,7]. Dyes cause a serious threat to water resources by severely affecting water quality parameters. Organic dyes are generally stable against changing effects and parameters such as light, chemicals, and heat. Most of them are also non-biodegradable [5]. It is known that the use of photocatalysis process, which is one of the advanced oxidation processes with advantages such as environmental friendliness and minimal energy consumption, is more promising for the removal of organic pollutants than traditional alternatives such as adsorption [5,8,9]. Basically, photocatalysis can be explained as the process of using a catalyst is used to accelerate degradation reactions through the action of UV or visible light. Of course, photocatalyst are the key to photocatalysis process. Photocatalysts are materials with existing and potential uses in the automotive, construction, consumer products, energy, environmental, mechanical, chemical, and medical sectors [9,10]. Many researchers report that the photocatalytic effect of

semiconductor nanomaterials used as catalysts can achieve effective results in the field of waste decomposition [5,11,12]. Today, nanostructured zirconia (ZrO_2), one of the most industrially important transition metal oxides, is used as a catalyst due to its excellent chemical and physical properties such as thermal stability, electrical properties, optical properties, chemical inertness and non-toxicity, as well as its high ion exchange capacity and redox activity [13–15]. This material has a wide band gap, which allows for structural modifications that can directly enhance catalytic activity through the presence of oxygen vacancies on the catalytic surface [8]. Owing to these properties, ZrO_2 is also widely used in many fields such as the automotive industry, electrical applications, construction, agriculture and energy. Various reports have been published in the literature on the use of ZrO_2 for the photodegradation of dyes and organic pollutants. All crystal forms of ZrO_2, monoclinic, tetragonal and cubic, can have photocatalytic properties [16]. Depending on the synthesis method, calcination temperature and synthesis parameters, products containing a combination of these phases can be obtained. It is thought that the presence of the tetragonal phase in the ZrO_2 structure, which is useful in various catalytic systems, indicates crystallographic rearrangement in the material due to oxygen vacancies and that the photocatalytic properties may be related to the trap levels present in the structure due to oxygen vacancies [17]. Vinayagam and co-workers synthesized zirconium oxide nanoparticles in tetragonal form with an energy band gap of 5.07 eV using a green reducing agent and achieved a methylene blue degradation efficiency of 89.11% [18]. Kumari et al. reported that ZrO_2 prepared by green methods and having more than 60% tetragonal phase achieved 81% photocatalytic efficiency at the end of 240 minutes for tetracycline, a pharmaceutical waste in water [19]. The 94.58% degradation efficiency of ZrO_2 synthesized by Saraswathi et al. for methyl orange, which has a predominantly tetragonal structure, was estimated to be due to the pure tetragonal structure [19,20]. In the light of this information, a study carried out by our team by conventional precipitation of zirconyl salts from aqueous solutions [21] investigated the synthesis conditions of ZrO_2 containing tetragonal phase and optimized the synthesis conditions for the smallest size material, which according to the literature is predicted to have the best morphology for photocatalytic applications. In this study, which is a continuation of the related study, the photocatalytic activity of the material synthesized using methylene blue as model pollutant was investigated.

2. Materials and Method

2.1 Materials

Zirconyl chloride octahydrate ($ZrOCl_2.8H_2O$, >98%) was obtained from ABCR; sodium hydroxide (NaOH) was obtained from Carlo Erba Reagenti; sulfuric acid (H_2SO_4, 95-97%) and hydrochloric acid (HCl, 37%) were obtained from Sigma-Aldrich and used without further purification.

2.2 Synthesis of ZrO_2 nanostructures

The ZrO_2 nanomaterial used in this study was synthesized by ultrasound-assisted method as in our previous study [21]. 0.1 M $ZrOCl_2.8H_2O$ was dissolved in 50 mL of distilled water. After mixing for 30 minutes to obtain a homogeneous solution, 5 M NaOH solution was added to the resulting solution to adjust the pH value to 10. Then, it was mixed in an ultrasonic bath at 70°C for 6 hours. The samples were then washed and collected by centrifugation at 9500 rpm for 15 minutes. Finally, the obtained samples were dried at 80°C overnight and calcined at 600°C for 2 hours.

2.3 Characterization of synthesized samples

Characterization of the synthesized products was carried out by Brunauer–Emmett–Teller (BET) surface area analysis, Zeta potential and UV-Vis absorption spectroscopy analysis. BET and Zeta potential analysis were carried out at Hitit University Scientific Technical Application and Research Center. For zeta potential measurements, the pH of the sample solutions prepared at 0.5 g/L concentration was adjusted to 2, 3, 4, 5, 6, 7, 8, 9 and 10 using 0.1 M HCl and 0.1 M NaOH. These solutions were kept in an ultrasonic bath for 1 hour and then mixed mechanically at 700 rpm for 19 hours at room temperature. The prepared samples were analyzed without waiting. BET surface area analysis was performed with Quantachrome/IQ-Chemi device using at least 100 mg sample. All samples were degassed in a degas unit under vacuum for 24 hours at 200°C. Specific surface areas were determined by a 5-point BET measurement with liquid nitrogen. Relative pressures (P/P_o) of 0.099, 0.150, 0.200, 0.250, and 0.300 were used for this analysis. For UV absorption spectroscopy analysis, the solutions of the sample was prepared with pH 7.4 buffer solution at a concentration of 0.5 g/L and mixed mechanically at 500 rpm for 5 min. Then, solution was prepared by a probe-type ultrasonic homogenizer for 10 min.

2.4 Photocatalytic activity

To determine the photocatalytic activity, the dye solution prepared under specified conditions by selecting methylene blue (MB) dye with a UV lamp with a wavelength of 366 nm was mixed in the dark for 10 min to reach the adsorption-desorption balance. In order to determine the effect of nanoparticle loading rate on photocatalytic degradation, ZrO_2 loadings were made in the range of 50-200 mg at 50 ml of 0.02 mM MB dye concentration for 90 minutes at room temperature. After optimizing the loading rate, the initial dye concentration in the range of 0.01-0.03 mM and the pH effect in the range of pH values 2-9 were examined. Kinetic study was carried out in the range of 0-120 min with a 254 nm wavelength UV lamp under conditions that provide the highest photocatalytic activity. In addition, under optimized conditions, the experiment was carried out under direct sunlight in the city of Çorum (geographic location 39 degrees 54 min. 20 sec. North Latitude and 34 degrees 04 min. 28 sec. East Longitude), on a sunny day on 03 July 2021, between 12.25 and 13.55 (outdoor temperature, 25–30 °C) was carried out. In addition, experiments were carried out

in different types of environments under the same conditions, under UV light of 366 nm wavelength, and in an ultrasonicator in order to determine the effect of sound waves. The amount of dye remaining without degradation in samples taken from a certain volume of dye solution containing ZrO_2 at different time intervals was determined by UV-Vis spectrometry. For all experiments, the dye degradation percentage was calculated with Equation 1 [22, 23]:

$$Dye\ Degredation = ((C_0 - C_t)/C_0) \times 100 \qquad (1)$$

where, C_0 is initial concentration of MB (ppm); C_t is concentration of MB at t time (ppm).

3. Analysis results

3.1. BET surface area and Zeta Potential measurement results

Increasing the surface area may be one of the factors responsible for increasing the photocatalytic activity of nanomaterials [24]. Therefore, BET surface area is an important analysis for photocatalytic studies. The BET surface area of the 9.24 nm sized ZrO_2 nanoparticle with 79% monoclinic and 21% tetragonal phase, synthesized under optimized conditions according to its size and morphology [21], was determined as 51.793 m^2/g. Navio and his colleagues reported that they obtained a surface area of 30 m^2/g for ZrO_2 powders of 5-50 μm sizes with tetragonal and monoclinic phases, which they synthesized using the sol-gel technique [25]. Hernández and his colleagues reported the surface area of ZrO_2 nanoparticles, which they synthesized with 7 nm size by hydrothermal method in an autoclave, as 44 m^2/g [26]. Singh and his colleagues also reported that they found the surface area of ZrO_2 nanoparticles of 50-60 nm in size, which they synthesized by hydrothermal method in an autoclave, to be 27 m^2/g [27]. Gionco and his colleagues also reported that the ZrO_2 nanoparticle they synthesized using a similar method had a surface area of 44 m^2/g [28]. García-Mendoza and his colleagues determined the surface area of ZrO_2 nanoparticles, which they synthesized with a size of 11.5 nm by the sol-gel method, as 73 m^2/g [29]. According to the literature research, ZrO_2 nanoparticles with a surface area above 50 m^2/g have been found in very few studies. It can be said that in this study, ZrO_2 nanoparticles with high surface area were synthesized by optimizing the synthesis method conditions.

The surface charge of metal oxide particles in aqueous solution is another important factor affecting the adsorption of molecules to the catalyst surface and possibly the degradation mechanism [30]. pH value strongly affects the surface charge properties of metal oxide particles in aqueous dispersion, the surface charges of both metal oxide particles and dye molecules depend on pH [30,31]. Therefore, determining the zero charge (isoelectric) point (PZC) is important to predict the charge on the nanoparticle surface during photocatalytic degradation of pollutants [32]. PZC indicates the pH value at which the surface charge is close to zero. In this case, the electrostatic interaction between the particle surface and the dye may be weak. Another important factor is the colloidal stability of

the suspensions. When the zeta potential value is close to zero, particles tend to aggregate as there is no electrostatic force to keep the particles apart. Therefore, it is important to determine this point [33]. Moreover, above the PZC, the surface of the particles has a negative net charge, while below the isoelectric point it has a positive net charge [30]. The stability of the synthesized ZrO_2 nanoparticles was analyzed by measuring the zeta potential in an aqueous system in the range of pH 2-9 using a deionized water suspension at room temperature. When metal oxide nanoparticles are dispersed in water or an organic solvent, –OH surface groups can be protonated or deprotonated, leading to the formation of $-OH_2^+$ or $-O^-$ surface charged groups, respectively [32]. Since the interaction between the photocatalyst surface and the dye is very important for process efficiency, zeta potential measurements as a function of pH were performed for photocatalyst suspensions of ZrO_2 nanoparticles and the results are shown in Figure 1.
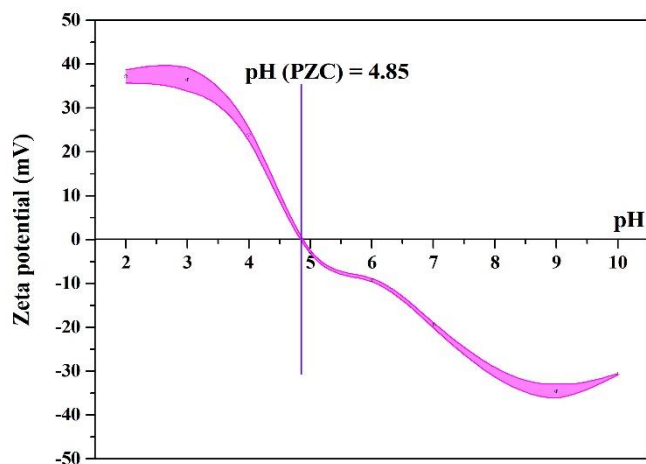

Fig. 1. Zeta potential measurements of ZrO_2 suspension in deionized water

It has been reported that the zeta potential range in unstable sols is generally between -30 and + 30 mV [34]. Zeta potential values observed for ZrO_2 nanoparticles at different pH range between +32.2±1.56 and -34.6±1.63 mV. These values are high and indicate particle stability in water and low agglomeration. The pH (PEP) value of 4.85 for ZrO_2 nanoparticles was found to be close to the results in the literature [25,35]. It is thought that the oxide surface can be strongly modified by hydrogen or hydroxyl ions in solution, as observed by the reversal of the zeta potential between pH 4.5 and 5.5. However, the interaction between two particles depends on the balance of electrical repulsion and van der Waals attraction. In aqueous solution, the surface charge of ZrO_2 varies as a function of pH. It is known that at low pH, the positive zeta potential of particles modifies the free surface energy of ZrO_2, reduces the thermodynamic barrier between tetragonal and monoclinic, and indicates the adsorption of H^+ ions [35].

3.2. UV-Vis Measurements

In photocatalysis, the optical band gap of the transition metal oxide plays a crucial role in determining its light-harvesting ability. Moreover, the reduction in nanoparticle size not only improves the band gap but also the surface area of nanomaterials, resulting in more efficient photodegradation performance [36]. For this reason, the UV-Vis spectrum of the ZrO_2 nanoparticle synthesized under optimized conditions was taken and given in Figure 2 (a). Absorption signals in the range of 200 to 300 nm arise from $O_2 \rightarrow Zr^{4+}$ charge transfer transitions with Zr in low coordination states [29]. In the UV−Vis spectroscopy graph, ZrO_2 nanoparticle showed a peak at 209 nm.

Reducing the size of nanomaterials shortens the charge recombination process by reducing the diffusion distance due to rapid charge transfer, resulting in improved photocatalytic efficiency [36]. Moreover, a larger band gap corresponds to stronger redox ability, leading to a decrease in the e/h + recombination rate and an improvement in photocatalytic activity. Since it is considered an electrochemical cell, the increase in band gap results in an increased oxidation-reduction potential [37]. The optical energy band gap of the ZrO_2 nanoparticle synthesized under optimized conditions was estimated by the Tauc plot (Figure 2(b)), in which the hv plot against $(\alpha h v)^2$ can be used, according to the Kubelka-Munk equation (Equation 2).

$$(\alpha h v)^2 = B(h v - E g) \tag{2}$$

Here, α is the absorption coefficient, h is the Planck constant, ν is the frequency of the photon, Eg is the optical energy band gap, and B is a constant [36,38]. To determine the optical bandgap value of the ZrO_2 nanoparticle, straight lines were drawn to fit the experimental curves and extended to intersect the (hv) axis [39]. Thus, the estimated optical energy band gap of the ZrO_2 nanoparticle synthesized under optimized conditions was determined as 3.062 eV. The band structures of ZrO_2 are highly dependent on the chemical microstructures, especially the crystal phases, crystal sizes and nature of defects. ZrO_2 contains three types of polymorphs: monoclinic, tetragonal and cubic. Theoretically, the valence band of ZrO_2 consists mainly of O 2p states with some mixing of Zr 4d states, and the conduction band consists mainly of Zr 4d states mixed with some O 2p states. The Zr 4d state in the conduction band is divided into two sub-bands upon the increasing symmetry of the crystal structure from monoclinic to tetragonal and cubic form [40]. It has been reported that the optical energy band gap of zirconia as a direct band gap insulator varies between 3.0 and 5.7 eV, and the low band gap may be related to oxygen deficiency in wide band gap semiconductors [41]. Navio et al. [22] reported an energy band gap of 3.65 eV for monoclinic ZrO_2 powders prepared by adding an aqueous solution of zirconium oxychloride and ferric nitrate to pH=9-10 and drying the gel at 600ºC.These authors argue that the decrease in band gap energy as a result of the conditions used in the sol–gel technique can be attributed to a highly disordered structure. As a result of structural defects, some energy levels are introduced into the semiconductor band gap, allowing lower

energy transitions, thus leading to a decrease in the band gap energy [42]. In our study, as seen in Table1, the estimated energy band gap of ZrO_2 nanoparticles synthesized under optimized conditions was found to be quite low compared to the literature.
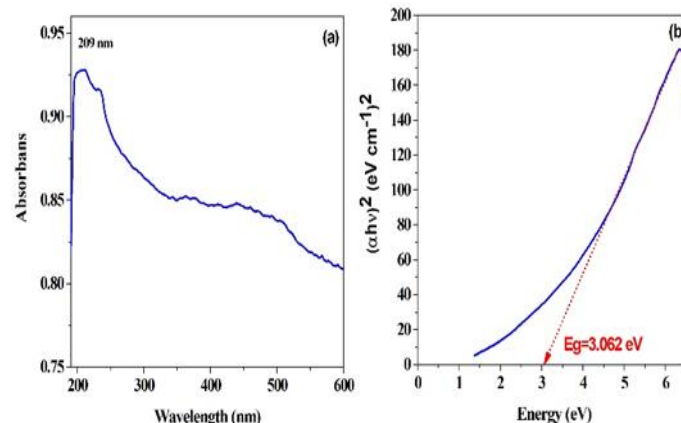

Fig. 2. a) UV–Vis spectrum of ZrO_2 nanoparticles, b) Tauc curve with Kubelka–Munk (K–M) function and estimated band gap of photocatalysis.

3.3. Photocatalytic activity measurements

MB, an organic cationic dye, was chosen for photocatalytic degradation studies due to its highly toxic nature in the environment. After dissolving in water, its molecules dissociate, releasing Cl-anions. When MB is dissolved in water, acid-base balance is not established because there is no available group to promote the hydrolysis reaction. Even the amino group, despite its basic behavior in water, does not promote hydrolysis as it is directly attached to an aromatic ring, greatly reducing its basicity (Kb ~ 10-9). This means that no change in solution pH is expected for MB solutions, meaning that the pH value for the solution should be close to the neutral pH value for deionized water [33]. For this reason, photocatalytic studies were started by using the natural pH value of 6.30 of the dye prepared in ultrapure water.

The photocatalytic degradation process is supported by catalyst dosage, which is an important parameter [43]. For this purpose, the amount of catalyst was changed between 0-200 mg by using 0.02 mM MB dye in ultrapure water at its pH of 6.30. In Figure 3 (a), the effect of the amount of catalyst on the degradation of MB dye is given, and it is seen that when 0, 50, 100, 150 and 200 mg ZrO2 nanoparticles are used (corresponding to 1, 2, 3 and 4 gL-1, respectively), degradation occurs at the rate of 3%, 49%, 63%, 91% and 94%, respectively. When the amount of photocatalyst is increased from 50 mg to 150 mg, it is seen that the photodegradation efficiency increases, which may be due to the increase in adsorbed photons and the presence of a large number of reactive sites on the catalyst surface [47].

Table 1. Comparison of the energy band gap of ZrO_2 nanoparticle prepared under optimum synthesis conditions with the literature

Crystal structure	Calcination temperature	Particle size	Eg (eV)	Ref.
Monoclinic	600	7 nm	4,83	[39]
Tetragonal	550	8 nm	4,4	[44]
Tetragonal	600	*	4,96	[38]
Tetragonal	450	<15 nm	4	[42]
Monoclinic	1100	<15 nm	3,5	
Monoclinic+Tetragonal	500	5-50 μm	3,65	[25]
Monoclinic	600	*	3,76	
Monoclinic	*	*	3,5	[45]
Tetragonal	*	*	3,9	
Monoclinic	**	50-60 nm	5,1	[27]
Monoclinic+Tetragonal	500	7 nm	5,15	[26]
Monoclinic+Tetragonal	**	*	5,15	[28]
Monoclinic+Tetragonal	**	34 nm	4,9	[41]
Tetragonal	**	17,6 nm	4,31	[46]
Tetragonal	600°C	29.25 nm	5.07	[18]
Monoclinic and Tetragonal	550°C	7 nm	2.85	[19]
Tetragonal	-	56.8 nm	-	[20]
Monoclinic+Tetragonal	400°C	50 nm	4.5-5	[8]
Monoclinic+Tetragonal	600	9,24	4,142	Current study

*: not determined, **: not done.

Further increases in catalyst above 150 mg appeared to have no significant effect on degradation efficiency. It has been reported in the literature for studies with different nanostructures that the reason for this may be the clustering of the particles of the material used as the catalyst, and that the clustering of these nanoparticles reduces the number of active sites on the catalyst. Moreover, these aggregated nanoparticles have been reported to act as scavengers for hydroxyl radicals [47]. However, degradation may be reduced at high doses due to the blocking effect of light penetration caused by the accumulation of excess catalyst solid particles. Therefore, it is necessary to determine the optimum amount of catalyst to enhance photodegradation through the production of e-/h+ pairs and subsequent large number of ·OH radicals [43]. According to these results, it was accepted that the maximum degradation efficiency was achieved for the 150 mg dosage of the catalyst.

Under optimized catalyst dosage conditions, degradation of different concentrations of MB dye (0.01, 0.02 and 0.03 mM) was carried out using ZrO_2 nanoparticles. When the dye concentration was increased threefold, a decrease in photocatalytic degradation efficiency was observed and the results are shown in Figure 3 (b). With ZrO_2 nanoparticles, MB was degraded by 83%, 91% and 73%, respectively, at MB dye concentration of 0.01, 0.02 and 0.03 mM (corresponding to 3.3, 6.7, 10 mgL-1, respectively). The maximum dye degradation achieved at 0.02 mM can be attributed to the fact that a greater number of active sites are available on the catalyst surface for degradation at the lowest contaminant concentration. Moreover, the surface area of the catalyst is such that it can adsorb a limited number of MB molecules. Beyond this limit, adsorption, and therefore degradation, decreases. In addition, at higher dye concentration, dye molecules can absorb light entering the mixture, thereby reducing the availability for catalyst activity [43]. When the concentration of the dye was 0.02 mM, a degradation efficiency of 91% was achieved, compared to a concentration of 0.03 mM, where the dye degradation efficiency decreased to 73%. Therefore, the above results suggest that ZrO_2 nanoparticles can be used as an effective photocatalyst for the degradation of organic dye even at high concentrations.

The photocatalytic efficiency of catalysts has a very significant impact due to the acid-base properties of the catalyst/fouling surfaces. Under acidic pH, vacancies are considered as the main oxidation species, while ·OH is considered as the main species at neutral or basic pH. However, the repulsion between the negatively charged surface of the photocatalyst and −OH in the basic environment affects the photodegradation efficiency. Agglomeration of the catalyst under acidic environment reduces the dye degradation activity by limiting the surface area [43]. Figure 3(c) shows the effect of pH value on the photocatalytic activity of ZrO_2 photocatalyst. It can be observed from Figure 3 (c) that pH value can significantly affect the photocatalytic activity of ZrO_2 photocatalyst. The degradation efficiency increases significantly from 1.4% to 91% with increasing pH value from 2 to 6.30, reaching a maximum of 91% at pH 6.30. The PZC and surface charge properties of ZrO_2 nanoparticles are related to changes in the pH of the solution. Because when the pH value is above the PZC, more cationic MB is absorbed onto the negatively charged photocatalyst surface. The PZC of ZrO_2 nanoparticles was determined as 4.85. However, when the pH value is increased to 10, the degradation efficiency decreases to 59%. This can be attributed to the instability of the photocatalyst in the strong alkaline state, as reported in the literature for
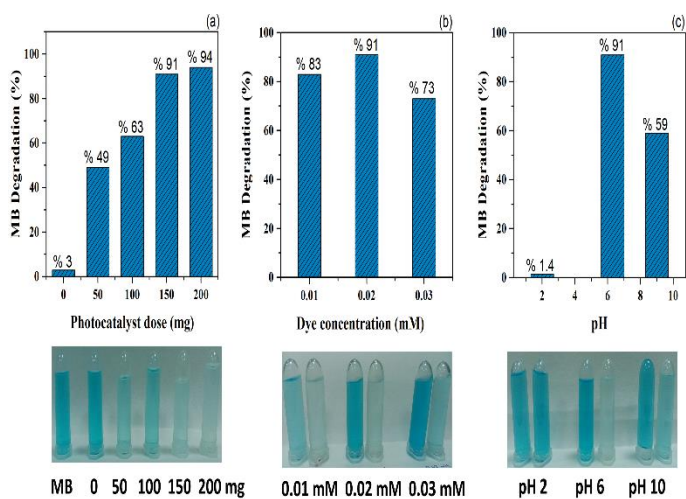
Fig. 3. Effect of (a) catalyst amount, (b) dye concentration and (c) pH on the photocatalytic activity of ZrO_2 nanoparticle.

different types of catalysts such as ZnO [48].

According to these results, the conditions with the highest photocatalytic activity of ZrO_2 nanoparticle were determined as 150 mg catalyst amount, 0.02 mM MB dye concentration and pH 6.30. The effect of 254 and 366 nm UV lamp wavelengths on the photocatalytic activity of ZrO_2 nanoparticle under optimized conditions was examined and given in Figure 4. The degradation kinetics of MB in the presence of ZrO_2 was analyzed using the Pseudo first-order kinetic model (Equation 3).

$$Ln(C_t/C_o)=kt \tag{3}$$

where C_o and C_t are the initial concentration of MB and its concentration at time (t), and k is the reaction rate constant (min-1) [49]. It can be seen that MB fragmentation at the 366 nm wavelength (91%) is higher than at the 254 nm wavelength (61%) and the rate constant is also 10 times larger.

In the degradation of MB, ZrO_2 nanoparticles were then tested in different configurations (photo and sonophotocatalysis) to compare the degradation performances of these different approaches. For visible irradiation, direct sunlight was used and the experiment was carried out in Çorum city (geographic location 39 degrees 54 min. 20 sec. North Latitude and 34 degrees 04 min. 28 sec. East Longitude) on a sunny day, between 12.25 and 13.55 on July 03, 2021. It can be seen from Figure 5 that during the photodegradation experiment with natural sunlight irradiation and UV light at a wavelength of 364 nm, a much higher degradation (87-91%) was achieved after 90 min than that obtained through sonocatalysis (76%). This indicates that under natural sunlight, the catalyst becomes photo-active due to the availability of sufficient energy for photodegradation [43].
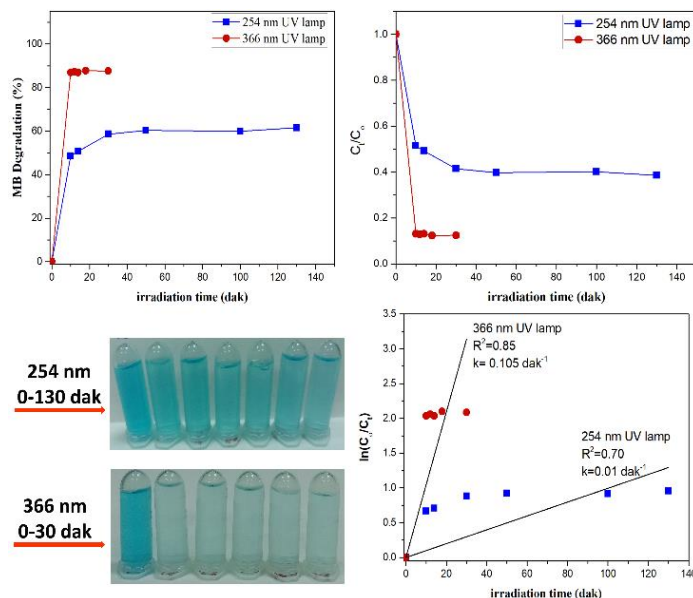

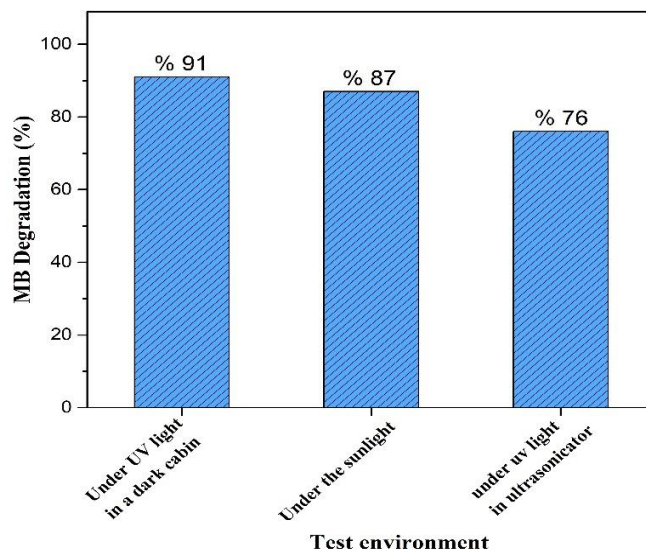Fig. 4. Effect of UV lamp wavelength on the photocatalytic activity of ZrO_2 nanoparticle

Fig. 5. Effect of test environment on the photocatalytic activity of ZrO_2 nanoparticle

A schematic diagram of load generation and transportation is shown in Figure 6. Under UV light, ZrO_2 nanoparticles are excited and photogenerated electrons move from the valence band (VB) to the conduction band (CB). The conduction band of ZrO_2 is more negative than that of $O_2/\cdot O_2^-$; therefore, while electrons can reduce O_2 to produce superoxide anions $\cdot O_2^-$, the valence band of ZrO_2 is not positive enough to oxidize OH^-/H_2O to form the active species $\cdot OH$. This indicates that MB dye is degraded mainly by active species $\cdot O_2$ and by accumulation of voids. Therefore, the enhanced photocatalytic degradation efficiency

can be attributed to the large number of hydroxyl ions in the alkaline environment, as mentioned above [32].

Table 2. Comparison of the photocatalytic performance of ZrO_2 nanoparticle synthesized under optimized conditions against MB with the literature

Samp.	Used Dye	Light Source	Catalysis Amount	Dye Degradation (%)	Ref.
Fe@ZrO₂ Ni@ZrO₂	MB (100 ppm, pH 11)	LED (100 W)	0.1 g	~ 95	[8]
MC-ZrO₂NPs	MB (10 ppm)	Under natural sunlight	0,25 g/L	~ 90	[18]
CZ05*	MB (7 ppm, pH 6,5)	LED lighting (400 nm)	3 g/L	~ 50	[28]
EZ05*	MB (7 ppm, pH 6,5)	LED lighting (400 nm)	3 g/L	~ 30	[28]
ZrO₂ (M)**	MB (10 ppm)	400W Xe lamps	1 g/L	~ 20	[27]
ZrO₂ nanofibers	MB (4 ppm)	UV lamp (254 nm)	0.01 g/L	38.47	[50]
ZrO₂ NPs	MB (10 ppm)	Xe lamp (400 nm)	0.01 g	~ 94	[51]
ZrO₂ (M/T)**	MB (10 ppm, pH 6,3)	366 nm UV light	3 g/L	73	***
ZrO₂ (M/T)**	MB (6,7 ppm, pH 6,3)	366 nm UV light	3 g/L	91	***

* Cerium (C) ve Erbium (E) Trace element doped ZrO_2 (Z)
M: monoclinic phase, T: tetragonal phase, *: current study

According to all the results obtained within the scope of the project, it can be seen from Table 2 that ZrO_2 nanoparticles synthesized under optimized experimental conditions exhibited high performance in the photodegradation of organic dye pollutant. Very few studies have been found in the literature investigating the photocatalytic activity of a single ZrO_2 nanoparticle. Generally, ZrO_2-based nanocomposites in combination with other metal oxides have been investigated, but as can be seen in Table 2, the photocatalytic activity of a single ZrO_2 nanoparticle has been examined for comparison purposes in very few studies. It is seen that the ZrO_2 nanoparticle synthesized by optimizing the synthesis conditions has high photocatalytic performance compared to various ZrO_2 nanostructures in the literature, based on the photocatalytic experimental procedure performed under similar conditions.
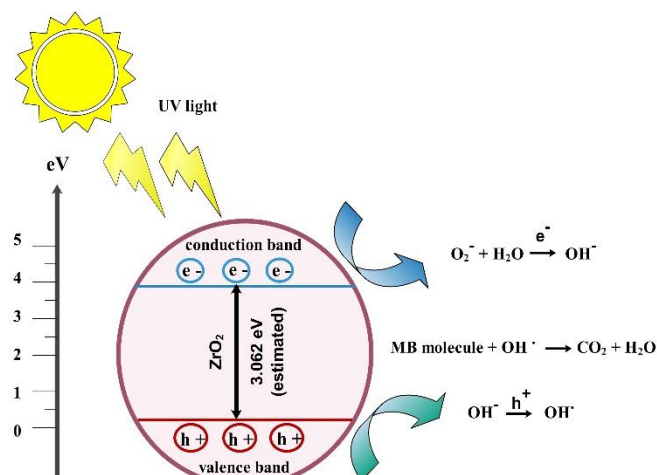

Fig. 6. Schematic illustration of the proposed photocatalytic mechanism of ZrO_2 nanoparticle under UV light irradiation.

4. Conclusions

The zeta potential, Brunauer–Emmett–Teller (BET) surface area and UV-Vis absorption spectrum of the ZrO_2 nanoparticle synthesized under optimized experimental conditions were analyzed. According to the zeta potential analysis results, high zeta potential values were observed for ZrO_2 nanoparticles in the range of +32.2±1.56 and -34.6±1.63 mV at different pHs, indicating particle stability in water and low agglomeration. From these data, the pH (PEP) value for ZrO_2 nanoparticles was determined as 4.85. According to BET surface area results, ZrO_2 nanoparticles were measured to have a specific surface area of 51,793 m^2/g.

With the data obtained from the UV-Vis absorption spectrum analysis results, Eg of ZrO_2 nanoparticles was estimated to be approximately 4.142 eV. Photocatalytic activity was evaluated by degradation of methylene blue under UV light (366 nm). The effect of varying the parameters such as 0, 50, 100, 150 and 200 mg catalyst amount, 0.01, 0.02 and 0.03 mM dye initial concentration and pH values of 2, 6, 30 and 9 of the dye solution, 366 and 254 nm wavelength of the UV light source used, type of test environment such as under UV light in dark environment, under UV light in sonicator, under UV light in mirrored cabinet and under direct sunlight on the removal efficiency of methylene blue was investigated. The highest removal efficiency was achieved in the dark chamber using 150 mg catalyst dosage, 0.02 mM MB solution, UV light source with 366 nm wavelength under pH 6.30 conditions, which is the pH of the dye in ultrapure water. When the UV light source with 254 nm wavelength was used, it was determined that the degradation rate was low and occurred more slowly. It was also observed that the reflection of UV rays had no significant effect on dye degradation using a mirrored booth.

The photocatalytic mechanism of ZrO_2 nanoparticle under UV light irradiation was proposed and a high degradation efficiency of 91% was achieved by providing a strong alkaline environment as a result of the formation of OH radicals with increasing concentration of hydroxyl ions of ZrO_2 nanoparticles. According to all the results obtained, it is predicted that the synthesised ZrO_2 nanoparticles can be successfully used for practical application in the photodegradation of organic paint pollutants. Although photocatalysis processes are a method that can overcome the treatment challenges for industries such as automotive and chemical, where wastewater problems are prominent, new developments are still needed in the preparation of sustainable and economically viable photocatalysts.

Acknowledgment

Conflict of Interest Statement

The authors declare that there is no conflict of interest in the study.

CRediT Author Statement

Filiz Boran: Conceptualization, Investigation, Methodology, Resources, Project administration, Supervision, Visualization, Writing–Original Draft, Writing – Review & Editing, **Mustafa Seyrek:** Investigation, Resources, Writing–Original Draft, Writing–Review & Editing, **Merve Okutan:** Investigation, Resources, Writing –Original Draft.

References

[1] Karagoz M, Uysal C. Environmental Pollution Cost Analyses of a Compression Ignition Diesel Engine Fuelled With Tire Pyrolytic Oil-Diesel Blends. Int J Automot Sci Technol. 2020;4(4):281-288.

[2] Hassan NS, Jalil AA, Khusnun NF et al. Extra-modification of zirconium dioxide for potential photocatalytic applications towards environmental remediation: A critical review. J Environ Manage. 2023;327:116869.

[3] Wang W, Lv Y, Liu H, Cao Z. Recent advances in application of polypyrrole nanomaterial in water pollution control. Sep Purif Technol. 2024;330:125265.

[4] Pirzada BM, Mir NA, Qutub N, Mehraj O, Sabir S, Muneer M. Synthesis, characterization and optimization of photocatalytic activity of TiO_2/ZrO_2 nanocomposite heterostructures. Mater Sci Eng B. 2015;193:137–145.

[5] Krishnan A, Swarnalal A, Das D, Krishnan M, Saji VS, Shibli SMA. A review on transition metal oxides based photocatalysts for degradation of synthetic organic pollutants. J Environ Sci. 2024;139:389–417.

[6] Mohtashami R, Shang JQ. Treatment of automotive paint wastewater in continuous-flow electroflotation reactor. J Clean Prod. 2019;218:335–346.

[7] Mohtashami R, Shang JQ, Xu Y. Treatment of automotive paint wastewater using electroflotation: kinetic study, influencing factors and data analysis. Environ Process. 2018;5(3):577–591.

[8] Khan K, Saeed M, Awad SA et al. Facile synthesis of zirconia supported nanomaterials for efficient photocatalytic applications. J Chinese Chem Soc. 2023;70(1):46–57.

[9] Kumari H, Sonia, Suman et al. A review on photocatalysis used for wastewater treatment: dye degradation. Water Air Soil Pollut. 2023;234:349.

[10] Nair K S, Manu B, Azhoni A. Sustainable treatment of paint industry wastewater: Current techniques and challenges. J Environ Manage. 2021;296:113105.

[11] Sampurnam S, Muthamizh S, Balachdran S, Narayanan V. Fabrication of hybrid polyaniline – Polyoxometalate decorated with ZrO_2 ternary nanocomposites with excellent visible light driven photocatalytic performance. J Photochem Photobiol A Chem. 2023;443:114844.

[12] Ramamoorthy S, Das S, Balan R, Lekshmi IC. Tuning donor-acceptor strength through preferential binding in mesoporous ZrO_2-TiO_2 nanocomposite as mechanistic approach for enhanced photocatalytic degradation of Alizarin Yellow GG dye. J Alloys Compd. 2022;898:162769.

[13] Ozkazanc H. Novel nanocomposites based on polythiophene and zirconium dioxide. Mater Res Bull. 2016;73(2):226–232.

[14] Teymourian H, Salimi A, Firoozi S, Korani A, Soltanian S. One-pot hydrothermal synthesis of zirconium dioxide nanoparticles decorated reduced graphene oxide composite as high performance electrochemical sensing and biosensing platform. Electrochim Acta. 2014;143:196–206.

[15] Sagadevan S, Podder J, Das I. Hydrothermal synthesis of zirconium oxide nanoparticles and its characterization. J Mater Sci Mater Electron. 2016;27(6):5622–5627.

[16] Majnis MF, Yee OC, Mohd Adnan MA, Yusof Hamid MR, Ku Shaari KZ, Muhd Julkapli N. Photoactive of Chitosan-ZrO_2/TiO_2 thin film in catalytic degradation of malachite green dyes by solar light. Opt Mater. 2022;124:111967.

[17] Basahel SN, Ali TT, Mokhtar M, Narasimharao K. Influence of crystal structure of nanosized ZrO_2 on photocatalytic degradation of methyl orange. Nanoscale Res Lett. 2015;10(1).

[18] Vinayagam R, Singhania B, Murugesan G et al. Photocatalytic degradation of methylene blue dye using newly synthesized zirconia nanoparticles. Environ Res. 2022;214:113785.

[19] Kumari N, Anand V, Sareen S et al. Synthesis of low-band gap porous zirconia nanoparticles via greener-route: Mechanistic investigation and their applications. Mater Chem Phys. 2023;294:127004.

[20] Sai Saraswathi V, Santhakumar K. Photocatalytic activity against azo dye and cytotoxicity on MCF-7 cell lines of zirconium oxide nanoparticle mediated using leaves of Lagerstroemia speciosa. J Photochem Photobiol B Biol. 2017;169:47–55.

[21] Boran F, Okutan M. Synthesis optimization of ZrO_2 nanostructures for photocatalytic applications. Turkish J Chem. 2023;47(2):448–464.

[22] Sultan M, Waheed A, Bibi I, Islam A. Ecofriendly reduction of methylene blue with polyurethane catalyst. Int J Polym Sci. 2019;2019: 3168618.

[23] Desai KR, Pathan AA, Bhasin CP. Synthesis, characterization of cadmium sulphide nanoparticles and its application as photocatalytic degradation of Congored. Int J Nanomater Chem. 2017;3(2):39–43.

[24] Seema H, Christian Kemp K, Chandra V, Kim KS. Graphene-SnO$_2$ composites for highly efficient photocatalytic degradation of methylene blue under sunlight. Nanotechnology. 2012;23(35).

[25] Navío JA, Hidalgo MC, Colón G, Botta SG, Litter MI. Preparation and physicochemical properties of ZrO$_2$ and Fe/ZrO$_2$ prepared by a sol-gel technique. Langmuir. 2001;17(1):202–210.

[26] Hernández S, Gionco C, Husak T et al. Insights into the sunlight-driven water oxidation by Ce and Er-doped ZrO$_2$. Front Chem. 2018;6:368.

[27] Singh H, Sunaina, Yadav KK, Bajpai VK, Jha M. Tuning the bandgap of m-ZrO$_2$ by incorporation of copper nanoparticles into visible region for the treatment of organic pollutants. Mater Res Bull. 2020;123:110698.

[28] Gionco C, Paganini MC, Giamello E, Sacco O, Vaiano V, Sannino D. Rare earth oxides in zirconium dioxide: How to turn a wide band gap metal oxide into a visible light active photocatalyst. J Energy Chem. 2017;26(2):270–276.

[29] García-Mendoza C, Oros-Ruiz S, Ramírez-Rave S, Morales-Mendoza G, López R, Gómez R. Synthesis of Bi$_2$S$_3$ nanorods supported on ZrO$_2$ semiconductor as an efficient photocatalyst for hydrogen production under UV and visible light. J Chem Technol Biotechnol. 2017;92(7):1503–1510.

[30] Lops C, Ancona A, Di Cesare K et al. Sonophotocatalytic degradation mechanisms of Rhodamine B dye via radicals generation by micro- and nano-particles of ZnO. Appl Catal B Environ. 2019;243(July 2018):629–640.

[31] Chen F, Zhao J, Hidaka H. Highly selective deethylation of Rhodamine B: Adsorption and photooxidation pathways of the dye on the TiO$_2$/SiO$_2$ composite photocatalyst. Int J Photoenergy. 2003;5(4):209–217.

[32] Vasiljevic ZZ, Dojcinovic MP, Vujancevic JD et al. Photocatalytic degradation of methylene blue under natural sunlight using iron titanate nanoparticles prepared by a modified sol-gel method. R Soc Open Sci. 2020;7(9).

[33] De Mendonça VR, Mourão HAJL, Malagutti AR, Ribeiro C. The role of the relative dye/photocatalyst concentration in TiO$_2$ assisted photodegradation process. Photochem Photobiol. 2014;90(1):66–72.

[34] Mohammadi MR, Fray DJ. Synthesis and characterisation of nanosized TiO$_2$-ZrO$_2$ binary system prepared by an aqueous sol-gel process: Physical and sensing properties. Sensors Actuators, B Chem. 2011;155(2):568–576.

[35] Arantes TM, Mambrini GP, Stroppa DG et al. Stable colloidal suspensions of nanostructured zirconium oxide synthesized by hydrothermal process. J Nanoparticle Res. 2010;12(8):3105–3110.

[36] Nazim M, Khan AAP, Asiri AM, Kim JH. Exploring Rapid Photocatalytic Degradation of Organic Pollutants with Porous CuO Nanosheets: Synthesis, Dye Removal, and Kinetic Studies at Room Temperature. ACS Omega. 2021;6(4):2601–2612.

[37] Wang X, Patel RL, Liang X. Significant improvement in TiO$_2$ photocatalytic activity through controllable ZrO$_2$ deposition. RSC Adv. 2018;8(45):25829–25834.

[38] Zhao J, Ge S, Pan D et al. Solvothermal synthesis, characterization and photocatalytic property of zirconium dioxide doped titanium dioxide spinous hollow microspheres with sunflower pollen as biotemplates. J Colloid Interface Sci. 2018;529:111–121.

[39] Keiteb AS, Saion E, Zakaria A, Soltani N. Structural and optical properties of zirconia nanoparticles by thermal treatment synthesis. J Nanomater. 2016;2016(4):1–6.

[40] Chang SM, Doong RA. Interband transitions in sol-gel-derived ZrO$_2$ films under different calcination conditions. Chem Mater. 2007;19(19):4804–4810.

[41] Peymani Forooshani R, Poursalehi R, Yourdkhani A. Optical and structural properties of colloidal zirconia nanoparticles prepared by arc discharge in liquid. AIP Conf Proc. 2018;1920:020028-1–020028-6.

[42] Herrera G, Montoya N, Doménech-Carbó A, Alarcón J. Synthesis, characterization and electrochemical properties of iron-zirconia solid solution nanoparticles prepared using a sol-gel technique. Phys Chem Chem Phys. 2013;15(44):19312–19321.

[43] Ciuparu D, Ensuque A, Shafeev G, Bozon-Verduraz F. Synthesis and apparent bandgap of nanophase zirconia. J Mater Sci Lett. 2000;19(11):931–933.

[44] Rani M, Shanker U. Sun-light driven rapid photocatalytic degradation of methylene blue by poly(methyl methacrylate)/metal oxide nanocomposites. Colloids Surfaces A Physicochem Eng Asp. 2018;559:136–147.

[45] Garcia JC, Scolfaro LMR, Lino AT et al. Structural, electronic, and optical properties of ZrO$_2$ from ab initio calculations. J Appl Phys. 2006;100(10).

[46] Hussain SA, Lkhayatt A, Adel H Omran, Mahdi EA. Effect of co-dopant on the structural and optical properties of nanocrystalline ZrO$_2$ thin films prepared by spray pyrolysis technique. J Appl Phys. 2016;8(5):44–49.

[47] Mahanthappa M, Kottam N, Yellappa S. Enhanced photocatalytic degradation of methylene blue dye using CuS–CdS nanocomposite under visible light irradiation. Appl Surf Sci. 2019;475:828–838.

[48] Lv T, Pan L, Liu X, Lu T, Zhu G, Sun Z. Enhanced photocatalytic degradation of methylene blue by ZnO-reduced graphene oxide composite synthesized via microwave-assisted reaction. J Alloys Compd. 2011;509(41):10086–10091.

[49] Wang Z, Srivastava V, Iftekhar S, Ambat I, Sillanpää M. Fabrication of Sb$_2$O$_3$/PbO photocatalyst for the UV/PMS assisted degradation of carbamazepine from synthetic wastewater. Chem Eng J. 2018;354:663–671.

[50] Zaborowska M, Smok W, Tanski T. Electrospinning synthesis and characterization of zirconia nanofibers annealed at different temperatures. Appl Surf Sci. 2023;615:156342.

[51] Chelliah P, Wabaidur SM, Sharma HP, Majdi HS, Smait DA, Najm MA, et. al. Photocatalytic organic contaminant degrada-tion of green synthesized ZrO$_2$ NPs and their antibacterial activities. Separations. 2023;10:156.